DOI: 10.1017/S1431927608086054
Microsc Microanal 14(Suppl 2), 2008
Copyright 2008 Microscopy Society of America

Controlling Channeling Effects in Aberration-Corrected STEM Tomography

Huolin L. Xin,* Varat Intaraprasonk** and David A. Muller**

* Department of Physics, Cornell University, Ithaca, NY 14853
** School of Applied and Engineering Physics, Cornell University, Ithaca, NY 14853

The short depth of focus in aberration-corrected STEM potentially could enable depth sectioning of nanoscale objects [1, 2]. In amorphous materials, the image is well described by the convolution of the three-dimensional (3D) point spread function (PSF) with the underlying 3D structure [3]. However channeling along zone-axis can render STEM-ADF through-focal series uninterpretable in crystalline samples [3-6]. Channeling breaks the linearity of the HAADF signal which is critical for a reliable reconstruction. However, Bals *et al* demonstrated that, in TEM, adding a 20mrad beam stop at the center of a 40-mrad objective aperture could reduce the thickness contrast [7]. By reciprocity, this suggests that introducing a beam stop in the center of the probe-forming aperture in STEM would efficiently suppress electron channeling as well. Loane and Silcox, about two decades ago, also discussed the impact of this geometry on the lateral PSF and lattice imaging in ADF STEM finding a tradeoff between improving the probe full-width at half maximum, at the expense of increased probe tails [8].

Here we report that the introduction of a 20-mrad beam stop at the center of the 50-mrad probe-forming aperture (Fig. 1(b)) of a 200 KeV C_5-corrected STEM (C_3 = -0.0096mm, C_5 = 3.85mm) would not significantly affect the resolution in all three dimensions, but can reduce the measured channeling effects significantly. It is a promising technique for obtaining interpretable C_5-corrected STEM Depth-sections.

Fig. 1(c-f) compares the PSF w/ and w/o the central-20-mrad beam stop. Fig. 1(e) demonstrates that the depth of focus is worse in the w/ beam stop case. However, for the lateral dimension of the probe at the peak-intensity defocus (Fig. 1(d)), the 20-mrad beam stop introduces a bigger side lobe but does not degrade the Scherzer resolution. These two arguments can be visually demonstrated in the reciprocal space as shown in Fig. 1(g, h), where the cross section of the 3D contrast transfer function (CTF) is plotted. It shows that the k_r-cutoff is the same for both cases. However, the cutoff along k_z is smaller for the w/ beam stop case consistent with the real-space result (Fig 1(e)). An analytical derivation shows that the k_z-cutoff is a function of only the semiangle of the beam stop (α_{min}) and the aperture (α_{max}), but not the aberrations. Further, the opening angles of the CTFs in the both cases are the same, implying the number of tilts needed in tilting tomography is not sacrificed when the central-20-mrad beam stop is introduced. This result is independent of accelerating voltage and aberrations.

Our Multislice simulation results (Fig. 2) show that inserting the beam stop efficiently suppresses channeling artifacts. Fig. 2(a-c) shows the depth sectioning of [110] Si with an embedded Hf atom, reconstructed by stacking 32 simulated through-focal ADF images together. Fig. 2(c) is the vertical profile through the left Si column. It qualitatively demonstrates that w/o the beam stop, an extra artifact peak is present, and adding the beam stop eliminates the artifact. Fig. 2(d-f) shows the probe (| |^2) propagation along a 55nm-thick [110] Si column. Fig. 2(f) compares the probe intensity along the Si column. It demonstrates that the electrons of w/-beam stop case leave the column quickly; whereas the electrons of the w/o-beam stop case remain strongly confined on the column, which is the source of the channeling artifacts.

References

[1] P. Batson, *Ultramicroscopy* **106** (2006), 1104-1114.
[2] K. van Benthem et al., *Ultramicroscopy* **106** (2006), 1062-1068.
[3] H. L. Xin et al., *Applied Physics Letters* **92** (2008), 013125.
[4] P. M. Voyles et al., *Ultramicroscopy* **96** (2003), 251-273.
[5] J. Einspahr, P. Voyles, *Ultramicroscopy* **106** (2006), 1041-1052.
[6] E. Cosgriff, P. Nellist, *Ultramicroscopy* **107** (2007), 626-634.
[7] S. Bals et al., *Ultramicroscopy* **104** (2005), 281-289.
[8] R. F. Loane, J. Silcox, *Proceedings of the 47th Annual Meeting of EMSA* (1989), 124.

[9] Research supported by Semiconductor Research Corporation

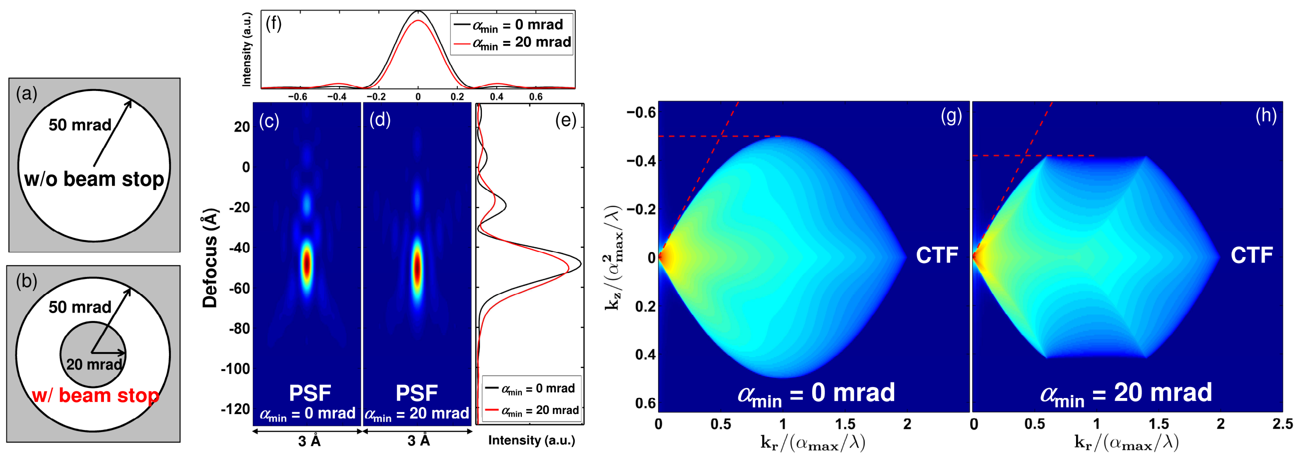

FIG. 1. Comparison of the 200 KeV aberration-corrected (α_{max} = 50 mrad) probe in both spatial and reciprocal space w/ and w/o the central-20-mrad beam stop: (a,b) Diagram of the probe-forming apertures used in our simulation. (c,d) The vertical cross section of the 3D PSF. (e) The vertical line profile through the middle of the PSF. (f) The lateral profile at the max-intensity defocus. (g,h) The cross section of the 3D CTF.

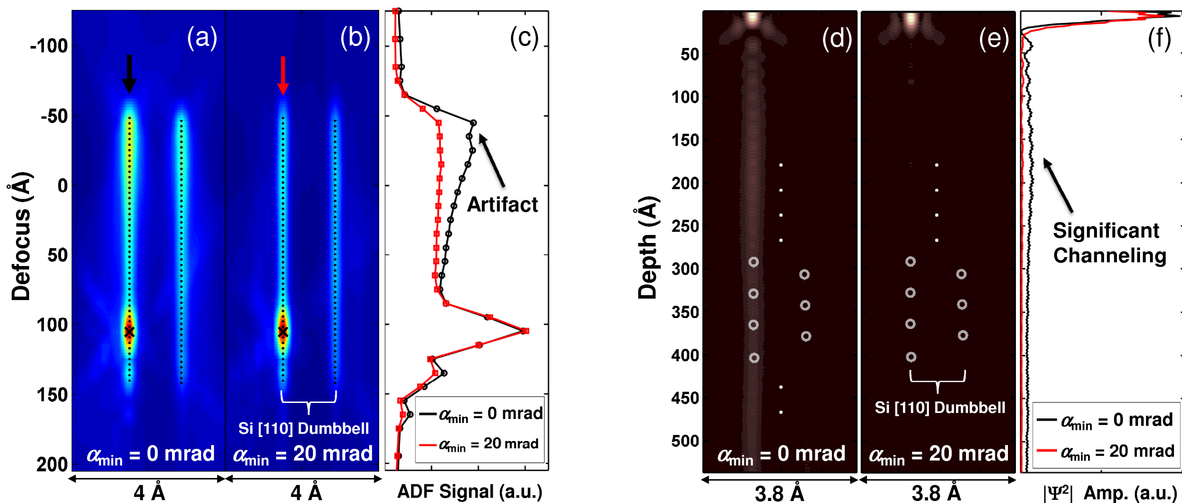

FIG. 2. Comparison of channeling effects w/ and w/o the central-20-mrad beam stop simulated by multislice method: (a-c) The depth sectioning of the 20nm-thick [110] Si with a Hf atom replacing a Si atom at Z = 153 reconstructed from a 32-image through-focal series. (d-f) The propagation of the probe (focused at the entrance surface on the left Si column) in a 55nm-thick [110] Si sample.